MARLEY

5/20/93

LECTURES ON RADIATIVE TRANSFER

I. GAS ABSORPTION

JIM POLLACK

EQUATION OF RADIATIVE TRANSFER

$$\mu \frac{dI}{d\tau} = I - S$$

μ = cosine of observer's $\measuredangle$

I = Specific Intensity
(energy flux in direction μ)

S = Source Function

τ = Optical depth.
(a measure of the probability of light interacting with gases and particles in path of Travel)

e = View $\measuredangle$

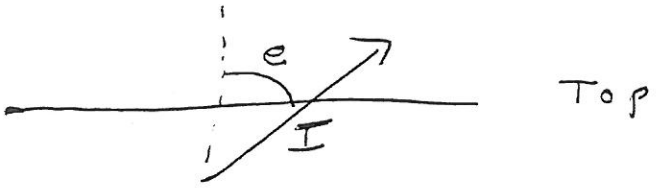

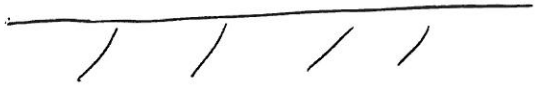

GAS OPACITY

NECESSARY CONDITION FOR ABSORTION/EMISSION:

Gas Molecule (or Atom) have a time varying electric (or magnetic) dipole (or higher order) moment

Example:

H_2O:

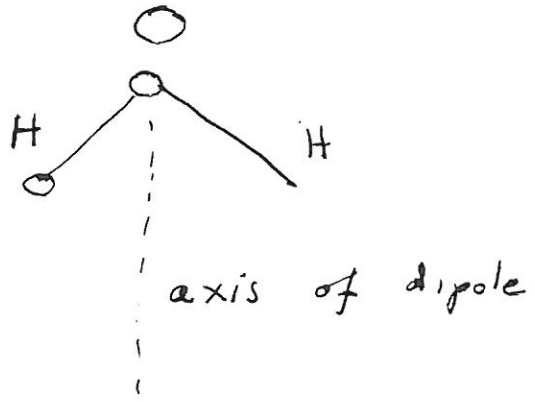

← ENERGY

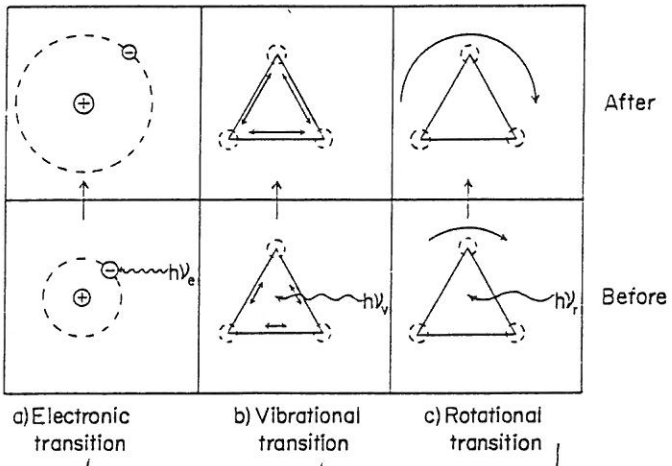

FIG. 8.1. Three kinds of atomic and molecular transitions that can occur upon absorption of a quantum of energy. The arrow lengths are proportional to the energy of vibration and rotation.

(λ) WAVELENGTH →

UV Near IR Far IR

~ .05 - .2 ~ 1 - 20 ~ 20 - 500 μm

← WAVE NUMBER ($\tilde{\nu}$) (cm^{-1})

~ 10^5 ~ 500 - 10,000 20 - 500

$$\tilde{\nu}\,(cm^{-1}) = \frac{1}{\lambda\,(cm)} = \frac{10^4}{\lambda\,(\mu m)}$$

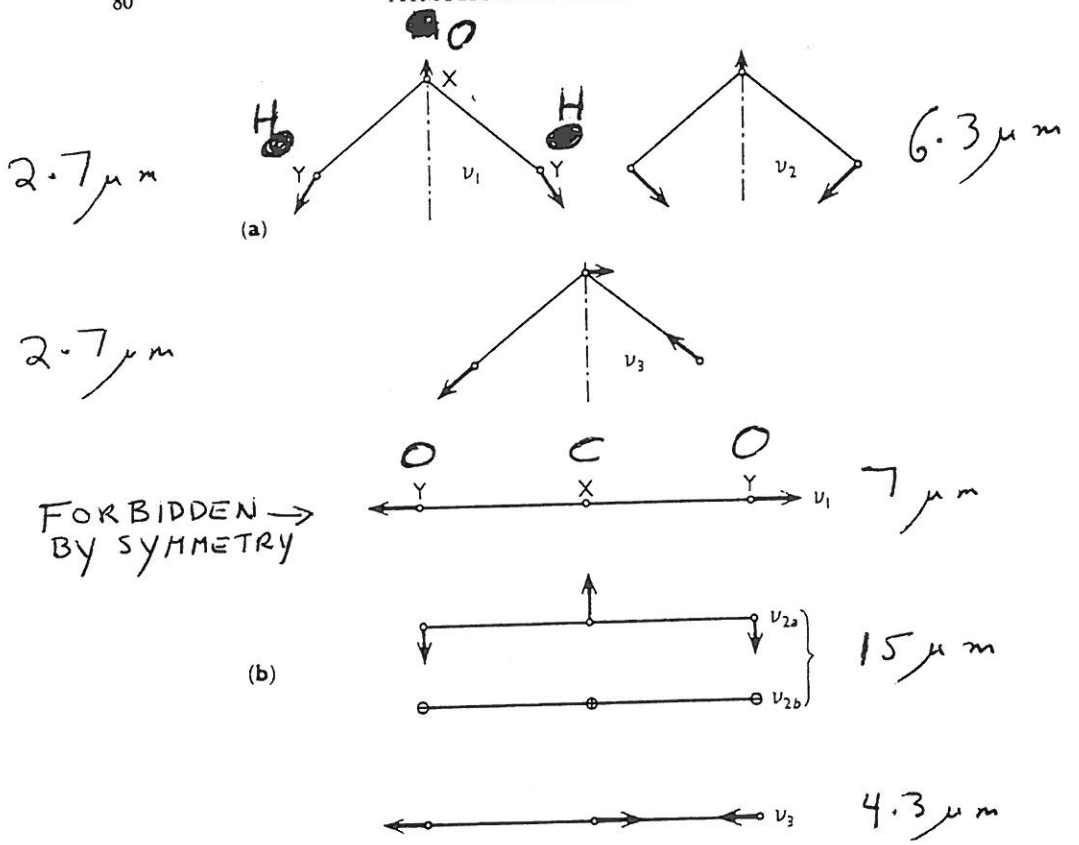

FIG. 3.9. Normal vibrations of a triatomic molecule. (a) H_2O is an example of a nonlinear triatomic molecule. (b) CO_2 is an example of a linear triatomic molecule. After Herzberg (1945).

Number of vibrational modes =
Total # degree of freedom (3 * # atoms)
– # Translational modes (= 3) — polyatomic
– # rotational modes (2 or 3) — diatomic

Ex: CO_2 – # vibr modes = 9 – 3 – 3 = 3

QUANTIZED ENERGY LEVELS

ROTATIONAL

– ENERGY LEVELS DEPEND ON MOMENTS OF INERTIA, I

$$E_r = h c F(J, K_A, K_C)$$

(h: Planck constant; c: speed of light)

$$F(J, K_A, K_C) = B J(J+1) + (A-B) K_A^2 + (C-B) K_C^2$$

$$A, B, C = h / 8\pi^2 c I_i$$

Ex :

CO_2 – Linear molecule → $A = B = C$

CH_4 – spherical top → $A = B = C$

NH_3 – symmetric top → $A \neq B = C$

H_2O – asymmetric top → $A \neq B \neq C$

O_3 – asymmetric top

– SELECTION RULES

permitted, dipole

$\begin{cases} \Delta J = +1 & \text{(rotational only)} \\ \Delta J = -1, 0, 1 & \text{(vibration + rotation)} \end{cases}$

~~LINE LOCATION~~

LINE LOCATIONS:

$$\Delta E_r = hc\tilde{\nu} = hc\ \Delta F$$

$$\longrightarrow$$

$$\tilde{\nu} = 2B_J(J+1)$$

(linear or spherical top)

VIBRATIONAL

Energy $$E_V = \sum_k hc\tilde{\nu}_k (V_k + 1/2)$$

↑ vibrational qt. #

Selection Rules $\Delta V_k = +n_k$ ← any integer

if $n_k = 1$ for $k = k^*$ & $= 0$ otherwise
fundamental

$n_k > 1$ for $k = k^*$ & $= 0$ otherwise
overtone

$n_k > 0$ for several k →
combination band

$\Delta J = \pm 1$

LINE LOCATIONS: $$\tilde{\nu} = \sum_k \tilde{\nu}_k n_k \pm 2B_J(J+1)$$

$\Delta J = 0$ → (or ≈ 0)

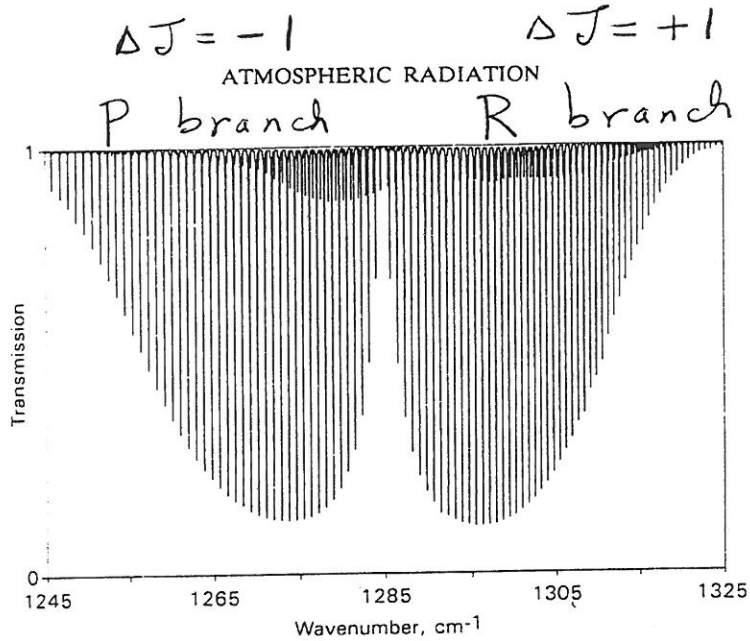

FIG. 3.3. Synthetic spectrum of N_2O near 7.78 μm. Spectral range: 1245–1325 cm^{-1}. Altitude of observation: 15 km. Zenith angle of observation: 30°. Terrestrial concentration ×1.

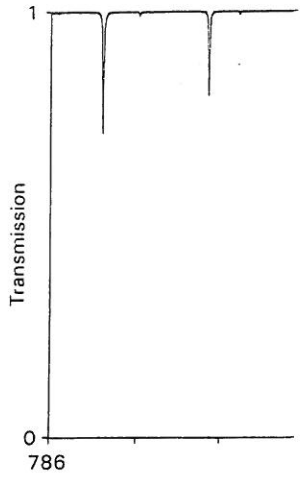

FIG. 3.5. Synthetic spectrum of C
Altitude of observation: 15 km. Zeni
×10.

Figure 3.2a and Fig. 3.2b are both centered on a region in the wing of the strong 3.31 μm band of methane. Figure 3.2a shows eight groups of lines (*manifolds*) while Fig. 3.2b shows details of one manifold. At the high dispersion of spectrum (b), each line is seen to have a finite width.

Figure 3.3 shows the central region of the strongest band of nitrous oxide. The two very regular g
the left and the right, respe
caused by a missing line at t
band is superimposed (an *upp*
center. Mixed in here, and als

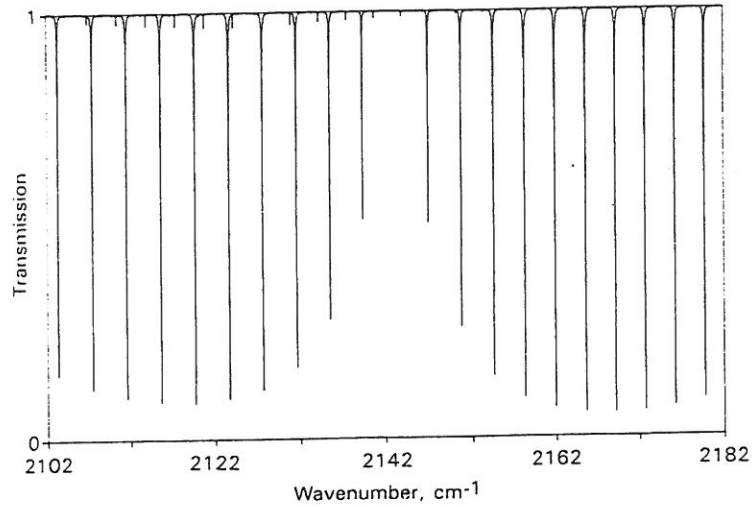

FIG. 3.4. Synthetic spectrum of CO near 4.67 μm. Spectral range: 2102–2182 cm^{-1}. Altitude of observation: 10 km. Zenith angle of observation: 30°. Terrestrial concentration ×1.

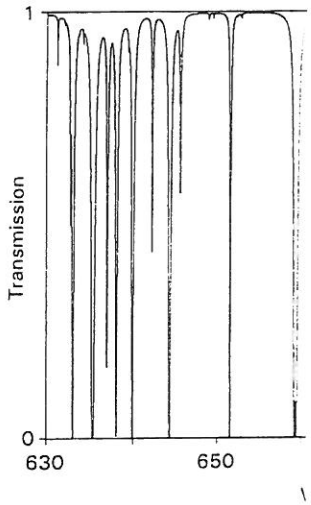

FIG. 3.6. Synthetic spectrum of H
Altitude of observation: 0 km. Zenith
×0.03.

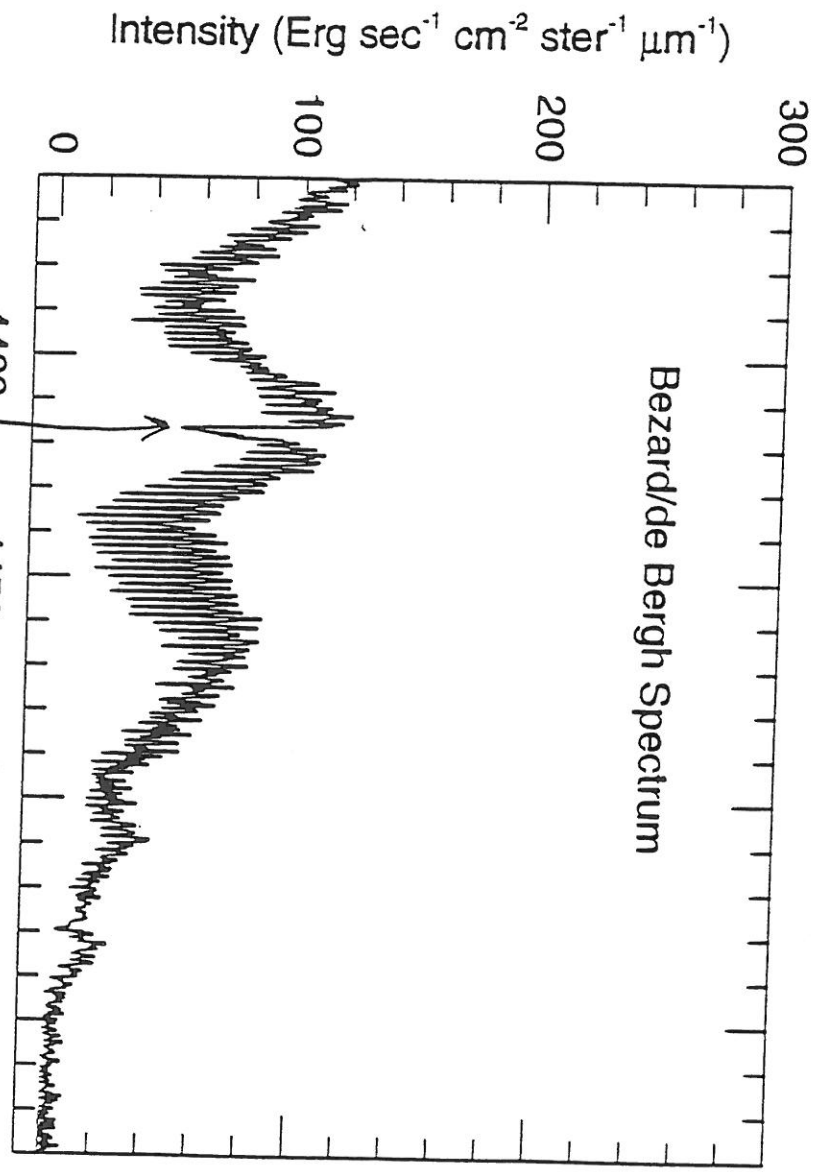
Intensity (Erg sec^{-1} cm^{-2} ster^{-1} μm^{-1})
0
100
200
300
Bezard/de Bergh Spectrum
4400
4450
4500
4550
Wavenumber (cm^{-1})
Q branch
ΔJ = 0

Fig. 10a

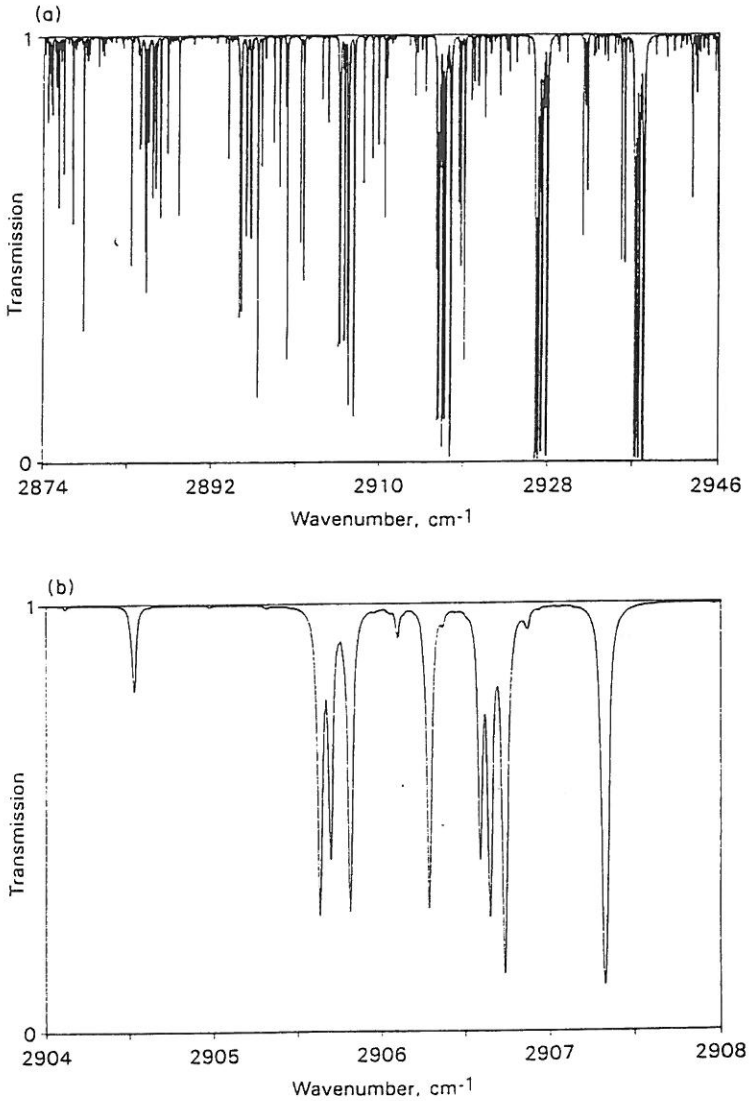

FIG. 3.2. Synthetic spectrum of CH_4 near 3.44 μm. Spectral range: (a) 2874–2946 cm^{-1}; (b) 2904–2908 cm^{-1}. Level of observation: 10 km. Zenith angle of observation: 30°. Terrestrial concentration ×1.

Each has been constructed by a computer for a single atmospheric constituent. The absorption path reaches from outside the atmosphere down to the level of observation at the given zenith angle of observation. Terrestrial gas concentrations are employed or a given multiple of them, if this makes for a clearer illustration.

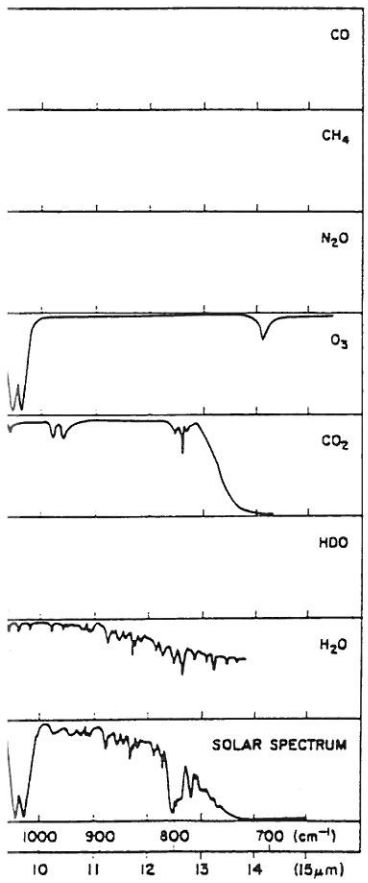

atmosphere. The top six panels are ies. The bottom panel is a simulated (1965).

ore complex theoretically but s shown in Fig. 3.1. Data for ical calculations are discussed

the form of discrete bands of ınd of water vapor, stretching all involve a change in the ering widths of the bands are rotational energy, and the *n bands.*

ɔtation bands at much higher .2, 3.3, 3.4, 3.5, 3.6, and 3.7.

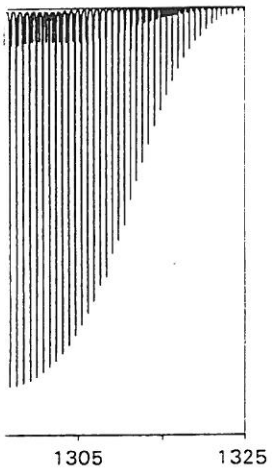

Spectral range: 1245–1325 cm^{-1}.
tion: 30°. Terrestrial concentration

ered on a region in the wing
ure 3.2a shows eight groups
tails of one manifold. At the
seen to have a finite width.
ne strongest band of nitrous

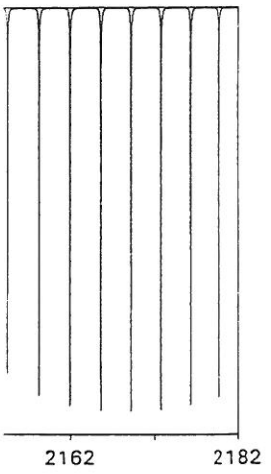

Spectral range: 2102–2182 cm^{-1}.
tion: 30°. Terrestrial concentration

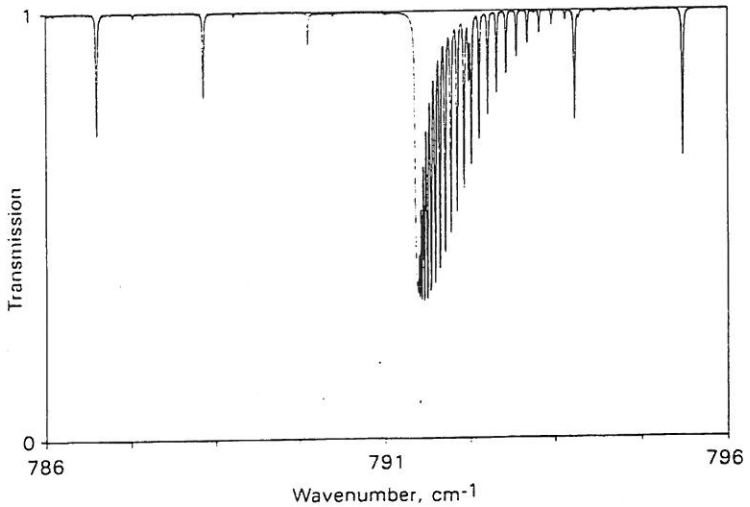

FIG. 3.5. Synthetic spectrum of CO_2 near 12.64 μm. Spectral range: 786–796 cm^{-1}. Altitude of observation: 15 km. Zenith angle of observation: 30°. Terrestrial concentration ×10.

oxide. The two very regular groups of lines are the *P- and R-branches* (to the left and the right, respectively) and they are separated by a gap caused by a missing line at the center of the band. A second, weaker band is superimposed (an *upper state band*) with a slightly different band center. Mixed in here, and also in most of the other spectra shown in this

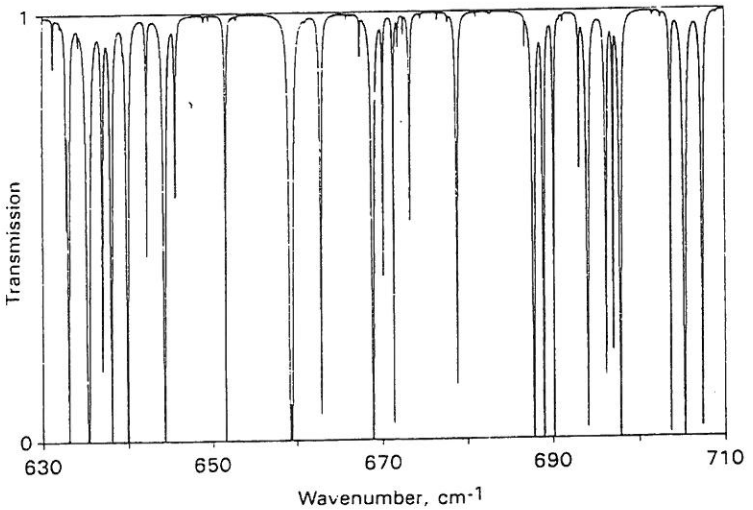

FIG. 3.6. Synthetic spectrum of H_2O near 14.9 μm. Spectral range: 630–710 cm^{-1}. Altitude of observation: 0 km. Zenith angle of observation: 30°. Terrestrial concentration ×0.03.

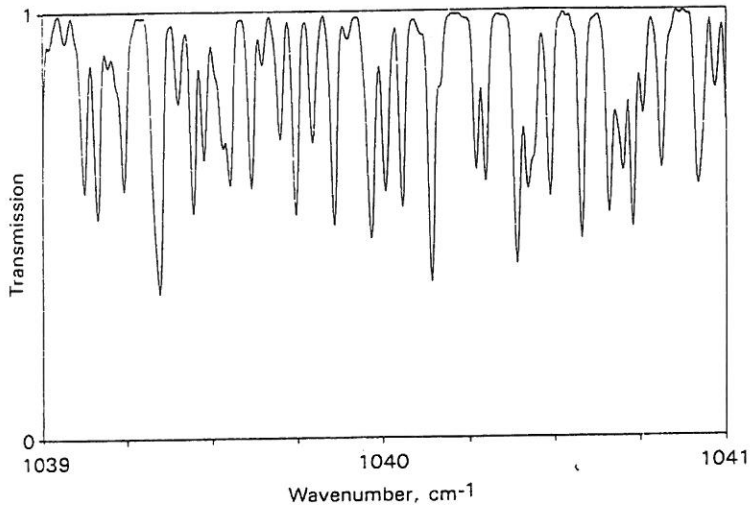

FIG. 3.7. Synthetic spectrum of O_3 near 9.61 μm. Spectral range: 1039–1041 cm^{-1}. Altitude of observation: 30 km. Zenith angle of observation: 30°. Terrestrial concentration ×1. Unlike most of the other synthetic spectra shown in this chapter, individual rotation lines are not resolved.

chapter, are weaker isotopic lines. In this spectrum, a few of the weak lines are from $^{14}N^{15}N^{16}O$.

Carbon monoxide, like nitrous oxide, is a linear molecule and the center of the 4.67 μm band shows a simple band structure (Fig. 3.4) similar to that in Fig. 3.3. The lines are more widely spaced than for nitrous oxide because the carbon monoxide molecule has a smaller moment of inertia. Again there is a gap in the band center (characteristic of a *parallel band*); a weak band of $^{13}C^{16}O$ is superimposed.

A high-resolution spectrum of a *perpendicular band* of a linear molecule is shown in Fig. 3.5. This is a weak band on the wing of the 15 μm band of carbon dioxide. It is the result of a transition involving two vibrational levels in close resonance (*Fermi resonance*), a circumstance that can greatly complicate the interpretation of a molecular spectrum. The P- and R-branches of this band are represented by the five, widely spaced, isolated lines. The gap between the bands is now filled with a partially resolved *Q-branch* near 790 cm^{-1}. Some weak isotopic lines of $^{16}O^{12}C^{17}O$ and $^{16}O^{12}C^{18}O$ are also present.

Figures 3.3, 3.4, and 3.5 illustrate arrays of lines containing some obvious order, but a glance at most regions of the atmospheric spectrum is more suggestive of a completely disordered situation. Figure 3.6 shows a region in the wing of the water vapor rotation band (this region is usually dominated by a very strong carbon dioxide band but the computer permits us to isolate species). The spectrum appears to be completely disordered, both as regards line positions and line intensities.

Figure 3.7 shows a sec
spectral resolution. The altit
above this level and the pres
§ 3.3.1); nevertheless, the
resolved. Each feature in
rotation lines.

3.2. Vibration–rotation sp

3.2.1. *The Hamiltonian for*

The quantum-mechanical
replacing variables by opera
E, of a system, consisting, ir
that make up a molecule.
equation is

We may separate the
independent terms,

H

(q represents the particle
states of the molecule from

This equation has discrete
functions, ψ_n. Transitions b
and emission of photons (fr

Provided that the time-
treated as a perturbation,
probability that a stationary

It is common practice
molecular energy, electroni
nuclear spin interactions, ea
and energy levels. The total
of energy, the wave func
functions, and emitted or a

2 CLASSES OF GAS ABSORPTION

- PERMITTED
  - — ISOLATED MOLECULE (ATOM) HAS TIME VARYING ELECTRIC (MAGNETIC) MOMENT
  - — SHARP SPECTRAL FEATURES
  - — GOOD ABSORBER AT LOW AND HIGH PRESSURES

- PRESSURE INDUCED
  - — REQUIRES A PAIR OF "COLLIDING" MOLECULES — ONE INDUCES AN ELECTRIC (MAGNETIC) MOMENT IN THE OTHER
  - — BROAD SPECTRAL FEATURES
  - — IMPORTANT ONLY AT HIGH PRESSURES

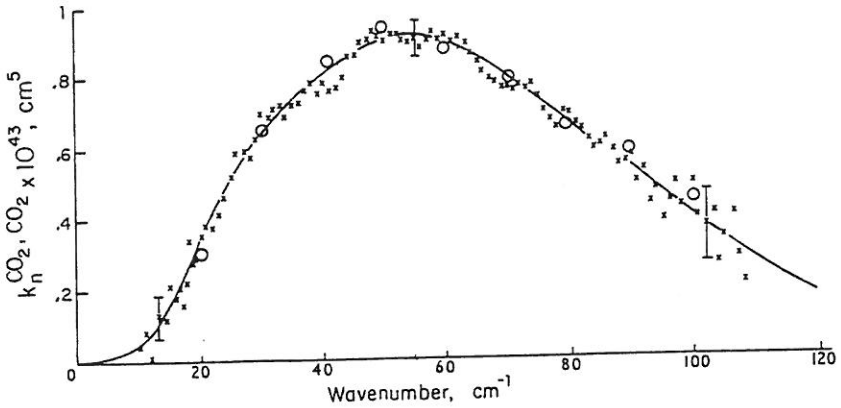

FIG. 5.10. The collision-induced rotation band of pure carbon dioxide at 293 K. The spectral resolution is 1.0 cm^{-1}. The circles and crosses are two independent sets of measurements. The vertical bars are error estimates. After Herries (1970).

CO_2 vs H_2O

CO_2 – NO PERMANENT DIPOLE MOMENT

→ NO PERMITTED PURE ROTATIONAL TRANSITIONS

H_2O – PERMANENT DIPOLE MOMENT

→ PERMITTED ROTATIONAL TRANSITIONS

CONTINUUM OPACITY

- BROAD ABSORPTION FEATURES
- SOURCE :
  - PRESSURE INDUCED TRANSITIONS
  - FAR WINGS OF LINES
  - DIMERS
- ABSORPTION COEFFICIENT, $\alpha_{\tilde{\nu}}$

$$\alpha_{\tilde{\nu}} = D_{\tilde{\nu}}(\tilde{\nu})\, F(T)\, P_b\, n_a$$

P_b = partial pressure of broadener

n_a = number density of absorber

$$\tau_{\tilde{\nu}} = \alpha_{\tilde{\nu}} L$$

L = path length

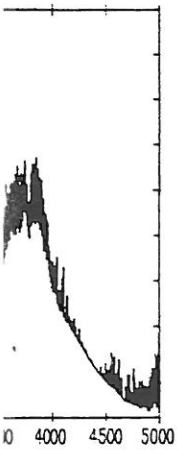

r vapor at 1 bar and 296 K. The
by a "radiation term,"

numbers) for $\nu/c > 500\ cm^{-1}$.

on coefficients, although
al coefficients with linear
ne thing. To attribute the
s is equivalent to saying
positioned close to band
and there are reasonable
he observed continuum

a theoretical line shape.
um; the fine structure by
lines; but, in fact, both
on line positions and line
a occur at all frequencies.
bsorption is stronger than
, but only the $1000\ cm^{-1}$

ption coefficients for the
ese are for water–water
coefficients for water–
he much larger concenta-
water–nitrogen collisions
view corresponds to that

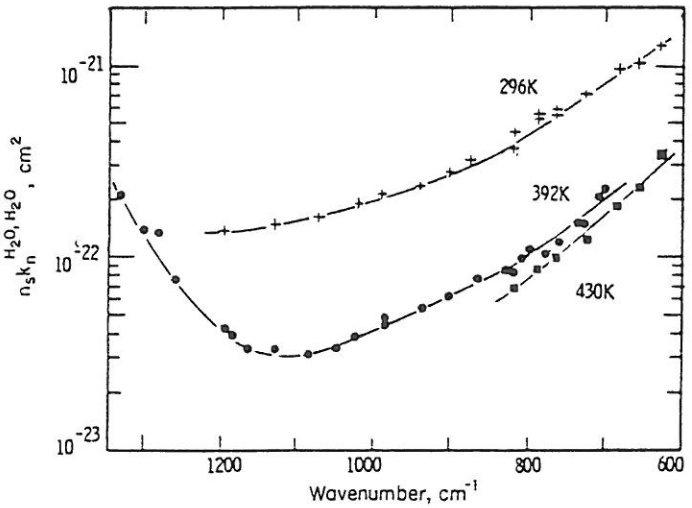

FIG. 5.8. Binary absorption coefficients for water–water collisions in the $1000\ cm^{-1}$ window. n_s is Loschmidt's number. After Burch and Gryvnak (1980).

of some field investigators, based on studies of the correlation between atmospheric absorption and water vapor pressure. The term *e-type absorption* (from the meteorological symbol for water vapor pressure) is often used to describe the self-broadening nature of this phenomenon.

The increase of absorption with decreasing temperature shown in Fig. 5.8 has been cited as a reason to favor dimer theories of the continuum, but this temperature variation is also consistent with far wing line shapes, given appropriate interaction potentials.

Figure 5.9 shows binary absorption coefficients in the $2600\ cm^{-1}$

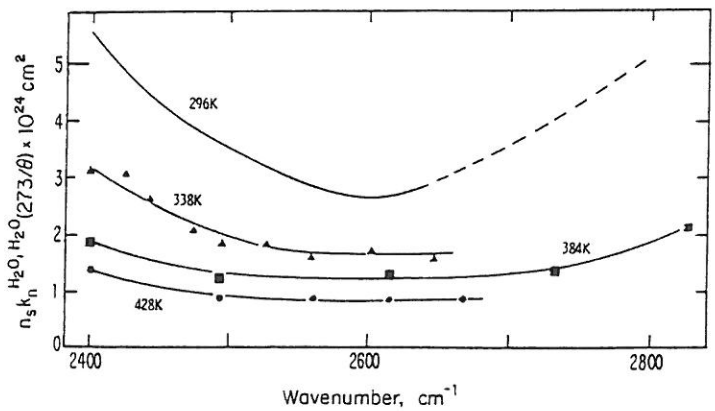

FIG. 5.9. Binary absorption coefficients for water–water collisions in the $2500\ cm^{-1}$ window. n_s is Loschmidt's number. The data for 296 K are extrapolated. After Burch and Gryvnak (1980).

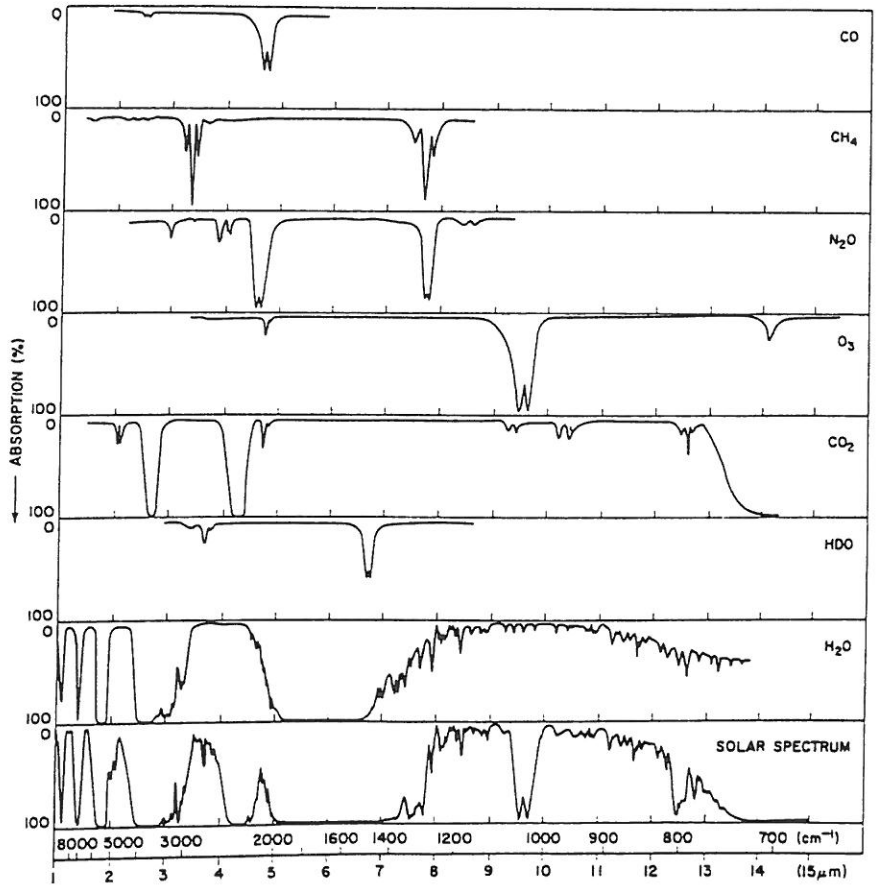

FIG. 3.1. Low-resolution absorption spectrum of the atmosphere. The top six panels are the absorption spectra of important atmospheric species. The bottom panel is a simulated absorption spectrum of the atmosphere. After Valley (1965).

be treated in this chapter since they are more complex theoretically but easier to handle empirically than the bands shown in Fig. 3.1. Data for electronic bands that are suitable for empirical calculations are discussed in Chapter 5.

The absorptions shown in Fig. 3.1 take the form of discrete bands of differing widths. Apart from the rotation band of water vapor, stretching from 16 μm to the microwave spectrum, all involve a change in the vibrational energy of the molecule. The differing widths of the bands are the result of simultaneous changes in the rotational energy, and the features are referred to as *vibration–rotation bands.*

The structures of selected vibration–rotation bands at much higher spectral resolution are illustrated by Figs. 3.2, 3.3, 3.4, 3.5, 3.6, and 3.7.

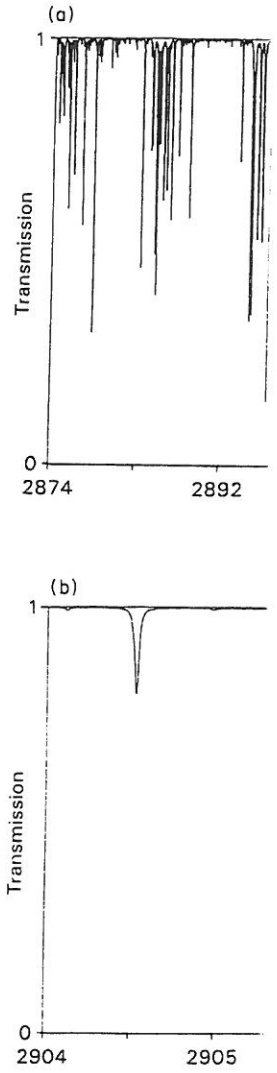

FIG. 3.2. Synthetic spectrum of
(b) 2904–2908 cm^{-1}. Level of c
Terrestrial concentration ×1.

Each has been constructe
constituent. The absorptior
down to the level of observ
Terrestrial gas concentratio
if this makes for a clearer il

LINE STRENGTH

$$S_L = S_L^\circ \quad W \quad F_R \quad F_V$$

S_L°: constant

W: weight (degeneracy factor)

F_R = fraction of molecules in INITIAL rotational energy level, J

F_V = fraction of molecules in initial vibrational state

$$W = \frac{(J+1)}{(2J+1)} \quad \text{for } J \rightarrow J+1 \text{ linear molecule}$$

molecules in the (v, J) level is the product of the fractions in the v level and the J level separately. From (2.45), (3.16), and (3.24)

$$F_{BV} = \frac{n(v)}{n} = Q_v^{-1} \exp\left(\frac{-v\mathbf{h}\nu}{\mathbf{k}\theta}\right), \tag{3.26}$$

where

$$Q_v = \sum_{v=0}^{\infty} \exp\left(\frac{-v\mathbf{h}\nu}{\mathbf{k}\theta}\right) = \left[1 - \exp\left(\frac{-\mathbf{h}\nu}{\mathbf{k}\theta}\right)\right]^{-1} \tag{3.27}$$

is the *vibrational partition function*, and

$$F_R = \frac{n(J)}{n} = Q_r^{-1}(2J+1) \exp\left[\frac{-B\mathbf{hc}J(J+1)}{\mathbf{k}\theta}\right], \tag{3.28}$$

where Q_r is the *rotational partition function*. Under normal atmospheric conditions, $B\mathbf{hc}/\mathbf{k}\theta \ll 1$ and

$$Q_r = \mathbf{k}\theta/\mathbf{hc}B. \tag{3.29}$$

Equations (3.16) and (3.18) are plotted as continuous functions of v or J in Figs. 3.13 and 3.14, and Table 3.2 gives populations of certain lowest excited vibrational states at two temperatures. The iodine molecule, illustrated in Fig. 3.13, has an unusually low vibrational frequency.

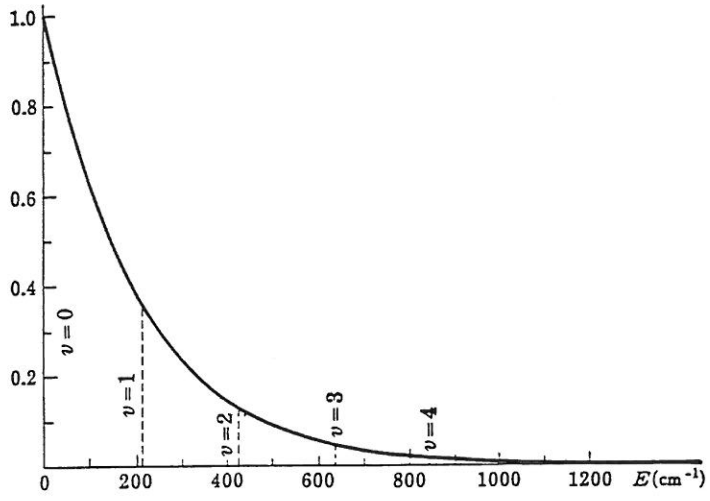

FIG. 3.13. Thermal distribution of vibrational levels. The data correspond to the iodine molecule, with $\nu_1 = 213.2\,\text{cm}^{-1}$, and for a temperature of 300 K. After Herzberg (1950).

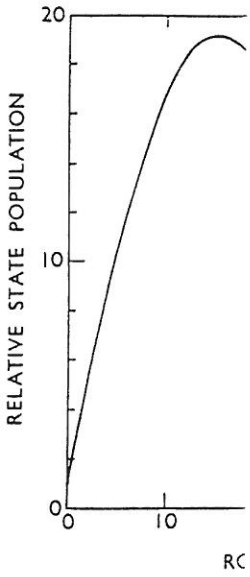

FIG. 3.14. Thermal distributior the same for all J. $B = 0.418$ cm

For most molecules at at first vibrational level is v The rotational states h approximately equal to

We have not consi

Table 3.2. Rat vibrational states

Gas	ν_1 (cm$^-$
H_2	4160.
HCl	2885.
N_2	2330.
CO	2143.
O_2	1556.
Cl_2	556.
I_2	213.

Source: After Herzb

of the fractions in the v level
.6), and (3.24)

$$\frac{h\nu}{\vartheta}\Big), \qquad (3.26)$$

$$\exp\Big(\frac{-h\nu}{k\theta}\Big)\Big]^{-1} \qquad (3.27)$$

$$\frac{hcJ(J+1)}{k\theta}\Big], \qquad (3.28)$$

. Under normal atmospheric

(3.29)

as continuous functions of v
gives populations of certain
peratures. The iodine mole-
ly low vibrational frequency.

1000 1200 $E(cm^{-1})$

The data correspond to the iodine
of 300 K. After Herzberg (1950).

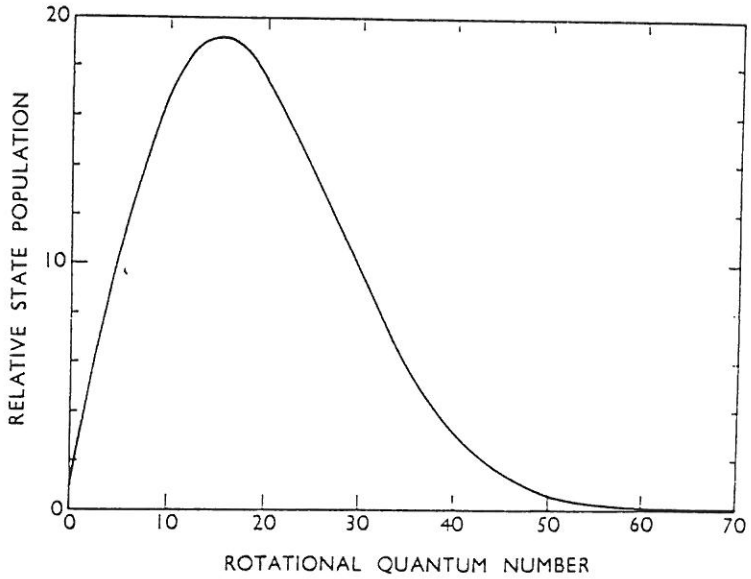

FIG. 3.14. Thermal distribution of rotational levels. The nuclear weights are assumed to be the same for all J. $B = 0.418\ cm^{-1}$ (nitrous oxide) and the temperature is 300 K.

For most molecules at atmospheric temperatures, the population of the first vibrational level is very small and varies rapidly with temperature. The rotational states have a maximum population for a J value approximately equal to

$$J_{max} = \Big(\frac{k\theta}{hcB}\Big)^{1/2} - \tfrac{1}{2}. \qquad (3.30)$$

We have not considered nuclear spins up to this point. They

Table 3.2. Ratio of the populations of the lowest two vibrational states for some molecules at 300 K and 1000 K

Gas	ν_1 (cm^{-1})	$\exp(-h\nu_1/k\theta)$ 300 K	$\exp(-h\nu_1/k\theta)$ 1000 K
H_2	4160.2	2.16×10^{-9}	2.51×10^{-3}
HCl	2885.9	9.77×10^{-7}	1.57×10^{-2}
N_2	2330.7	1.40×10^{-5}	3.50×10^{-2}
CO	2143.2	3.43×10^{-5}	4.58×10^{-2}
O_2	1556.4	5.74×10^{-4}	1.07×10^{-1}
Cl_2	556.9	6.92×10^{-2}	4.49×10^{-1}
I_2	213.2	3.60×10^{-1}	7.63×10^{-1}

Source: After Herzberg (1950).

LINE SHAPE

— Monochromatic absorption coefficient

$$k_{\tilde{\nu}} = S_L \, f(\tilde{\nu} - \tilde{\nu}_0)$$

$\tilde{\nu}_0$: line center; $f(\tilde{\nu} - \tilde{\nu}_0)$: line shape; S_L: line intensity

— Reasons for finite line extent

— Uncertainty Principle

Lorentz Line shape ⟶

$$f(\tilde{\nu} - \tilde{\nu}_0) = \frac{\alpha}{\pi\left[(\tilde{\nu} - \tilde{\nu}_0)^2 + \alpha^2\right]}$$

$$\alpha_Q = \frac{1}{2\pi c \, \tilde{\tau}_Q}$$

$\tilde{\tau}_Q$: Lifetime of excited state

— Collisions

$$\alpha = \frac{1}{2\pi c \, \tilde{\tau}_c}$$

$\tilde{\tau}_c$ = Time between collisions (permitted Transition)
= Time during Collision (pressure-induced)

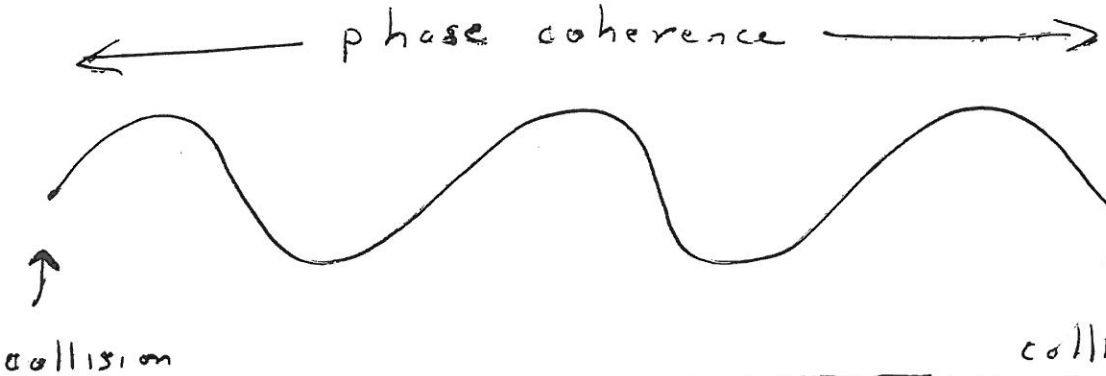

permitted :

$$\alpha_L \cong \frac{1}{c}\, n_b \sqrt{\frac{2kT}{\pi}\left(\frac{1}{m_b}+\frac{1}{m_a}\right)}$$

relative velocity from kinetic theory

(in reality - $\alpha_L \propto T^n$)

— Doppler shift

$$f_D(\tilde{\nu}-\tilde{\nu}_0) = \left(\frac{1}{\alpha_D \pi^{1/2}}\right) \exp\left\{-\left[\frac{(\tilde{\nu}-\tilde{\nu}_0)}{\alpha_D}\right]^2\right\}$$

$$\alpha_D = \left(\frac{\tilde{\nu}_0}{c}\right)\left(\frac{2kT}{m_a}\right)^{1/2}$$

— Comparison of half widths

$\alpha_Q << \alpha_D$

$\alpha_Q << \alpha_L$ (unless $P <<< 1$)

$\alpha_L > \alpha_D$ $P(mb) \gtrsim (1-10)$

$\alpha_D > \alpha_L$ $P(mb) \leq (1-10)$

LINE DATABASES FOR PERMITTED TRANSITIONS

— CONTAIN

various molecules
various Transitions

- $\tilde{\nu}_0$ – POSITION OF LINE CENTER
- S_L – LINE STRENGTH (T_{ref})
- α_L – PRESSURE HALF WIDTHS (T_{ref}, n, broadener)
  - n ↳ temperature exponent
- E_{Low} – Energy of lower level of a Transition

— EXAMPLES

Air Force Geophysical Lab

HITRAN – Put out by AFGL
Earth oriented

GEISA – French, Earth + outer Planets

HIGH T – diatomics, CO_2, H_2O] customized
For high Temperatures
(Venus, rocket plumes, cool stars)

CORRELATED k DISTRIBUTION

— DEFINITION:

PROBABILITY DISTRIBUTION OF MONOCHROMATIC ABSORPTION COEFFICIENTS IN FINITE SPECTRAL INTERVAL AT A GIVEN P, T

— MOTIVATION:

- NEED LARGE NUMBER OF MONOCHROMATIC CALCULATIONS IF DO THEM BY BRUTE FORCE

e.g. STP, $\alpha_L \sim 10^{-1}\ cm^{-1}$

if $\Delta\tilde{\nu} = 100\ cm^{-1}$

$\rightarrow \sim (10) \times 10^2 / 10^{-1} = 10^4$ calculations

(10 = # pts/half width)

— BASIC ASSUMPTIONS:

- EXACT ~~POINT~~ WAVENUMBER POSITION NOT IMPORTANT, SINCE SOURCE FUNCTIONS (SUNLIGHT, THERMAL RADIATION) VARY SLOWLY WITH $\tilde{\nu}$

- VERY SIMILAR SETS OF WAVELENGTHS HAVE ~~THE SAME~~ $k_{\tilde{\nu}}$ AT VARIOUS LEVELS IN THE ATMOSPHERE

DERIVATION

$$T_r(\Delta\tilde{\nu}) = \int_{\Delta\tilde{\nu}} e^{-k_{\tilde{\nu}} u} \frac{d\tilde{\nu}}{\Delta\tilde{\nu}}$$

absorber gas amount

T_r: transmission thru constant P, T

$$= \int e^{-k_{\tilde{\nu}} u} n(k)\, dk$$

$n(k)\,dk$ = probability of having an absorption coefficient between k and $(k + dk)$

Let $g(k) = \int_0^k n(k)\, dk$

$g(k)$: cumulative probability absorption coefficient $\leq k$

$$\rightarrow T_r(\Delta\tilde{\nu}) = \int e^{-k(g) u} dg$$

$$= \sum_i W_i e^{-k(g_i) u}$$

W_i: gauss weight; g_i: gauss point

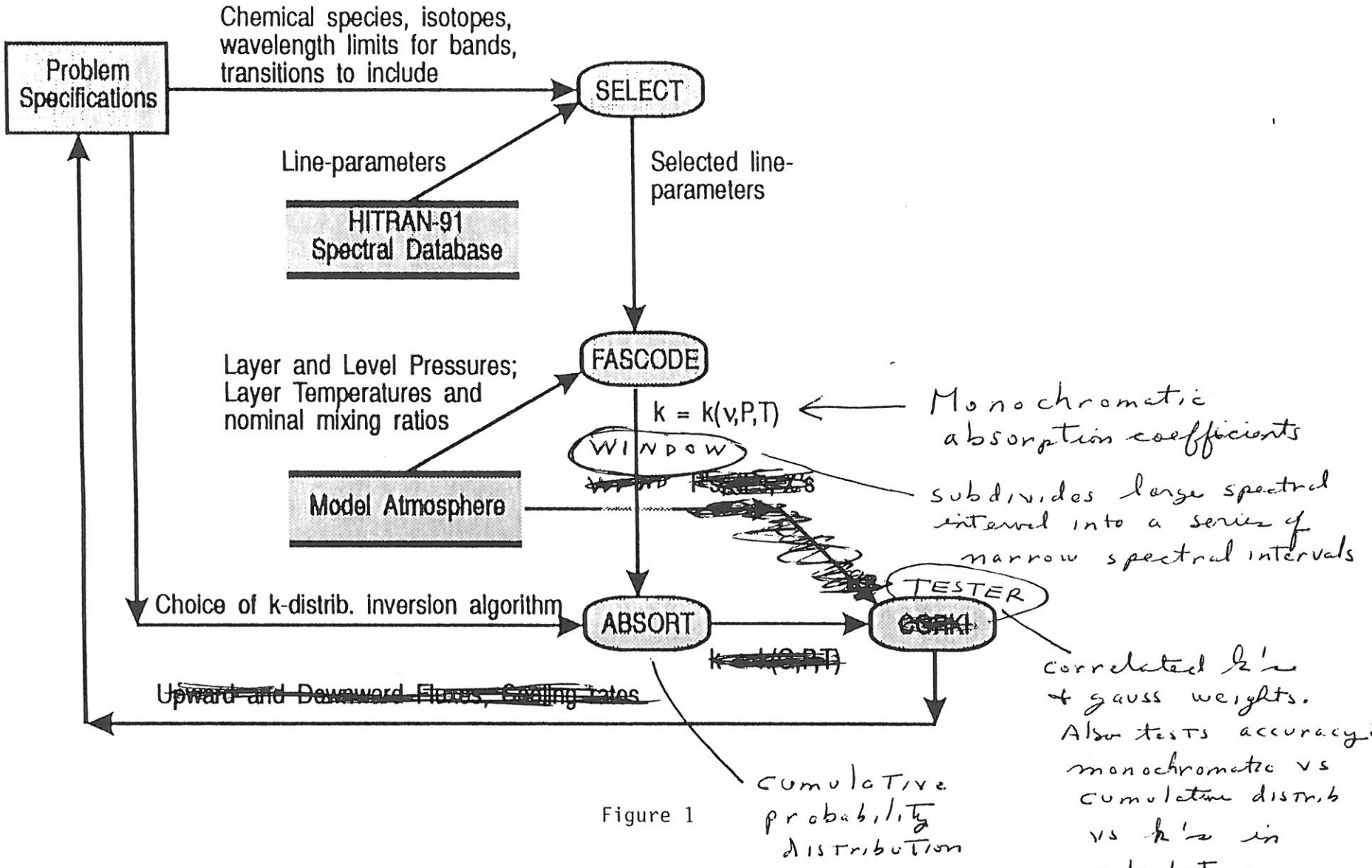
Problem Specifications
Chemical species, isotopes, wavelength limits for bands, transitions to include
SELECT
Line-parameters
HITRAN-91 Spectral Database
Selected line-parameters
FASCODE
Layer and Level Pressures; Layer Temperatures and nominal mixing ratios
k = k(ν,P,T)
Monochromatic absorption coefficients
WINDOW
subdivides large spectral interval into a series of narrow spectral intervals
Model Atmosphere
TESTER
Choice of k-distrib. inversion algorithm
ABSORT
correlated k's + gauss weights. Also tests accuracy: monochromatic vs cumulative distrib vs k's in calculating transmission
cumulative probability distribution

Figure 1

CH_4

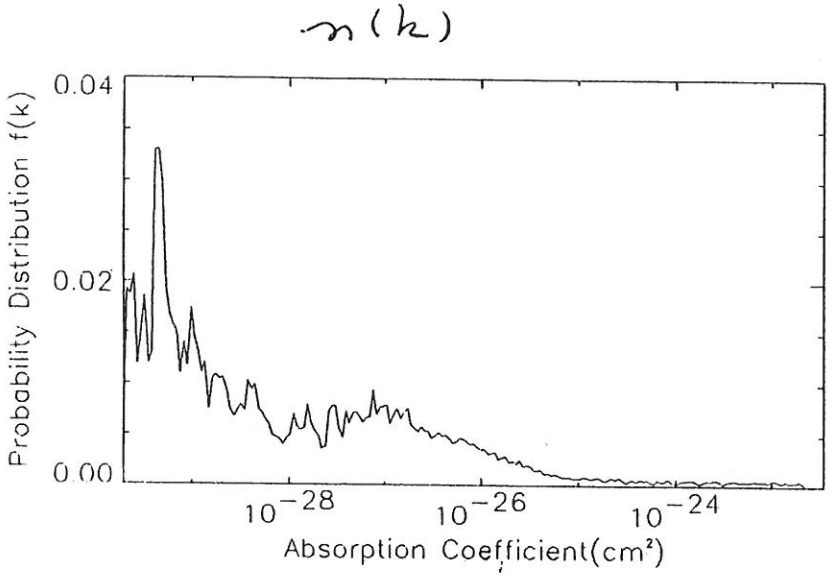

(a)

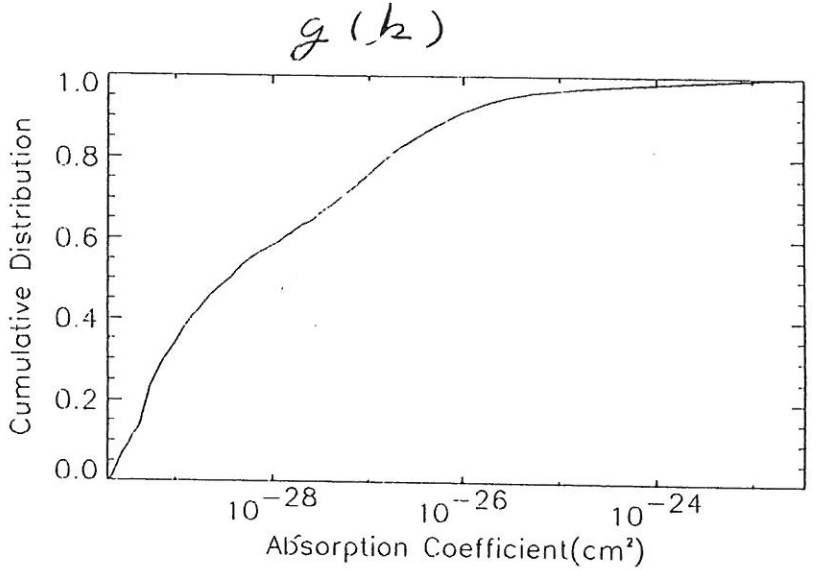

(b)

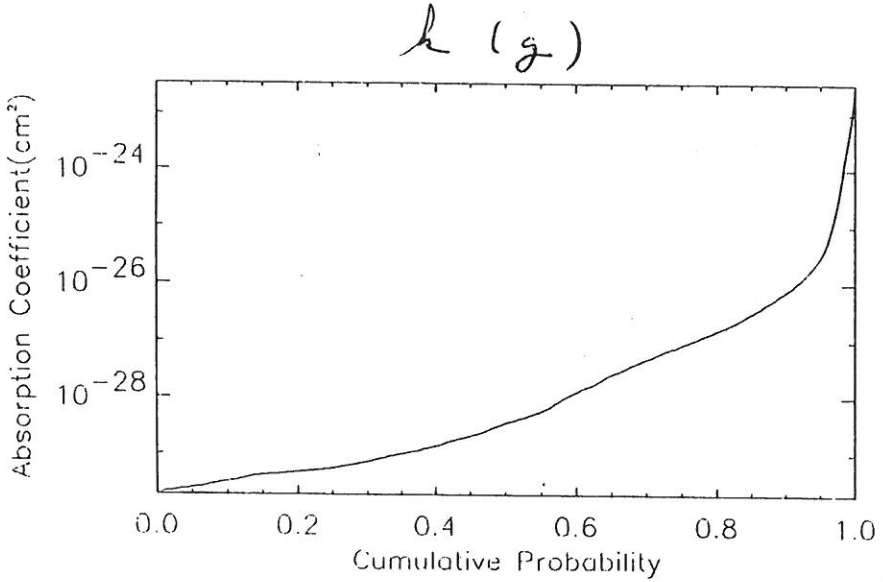

(c)

Pressure	1.480 bar
Temperature	272.23
Band Low	1300.0
Band High	1320.0

Figure 2

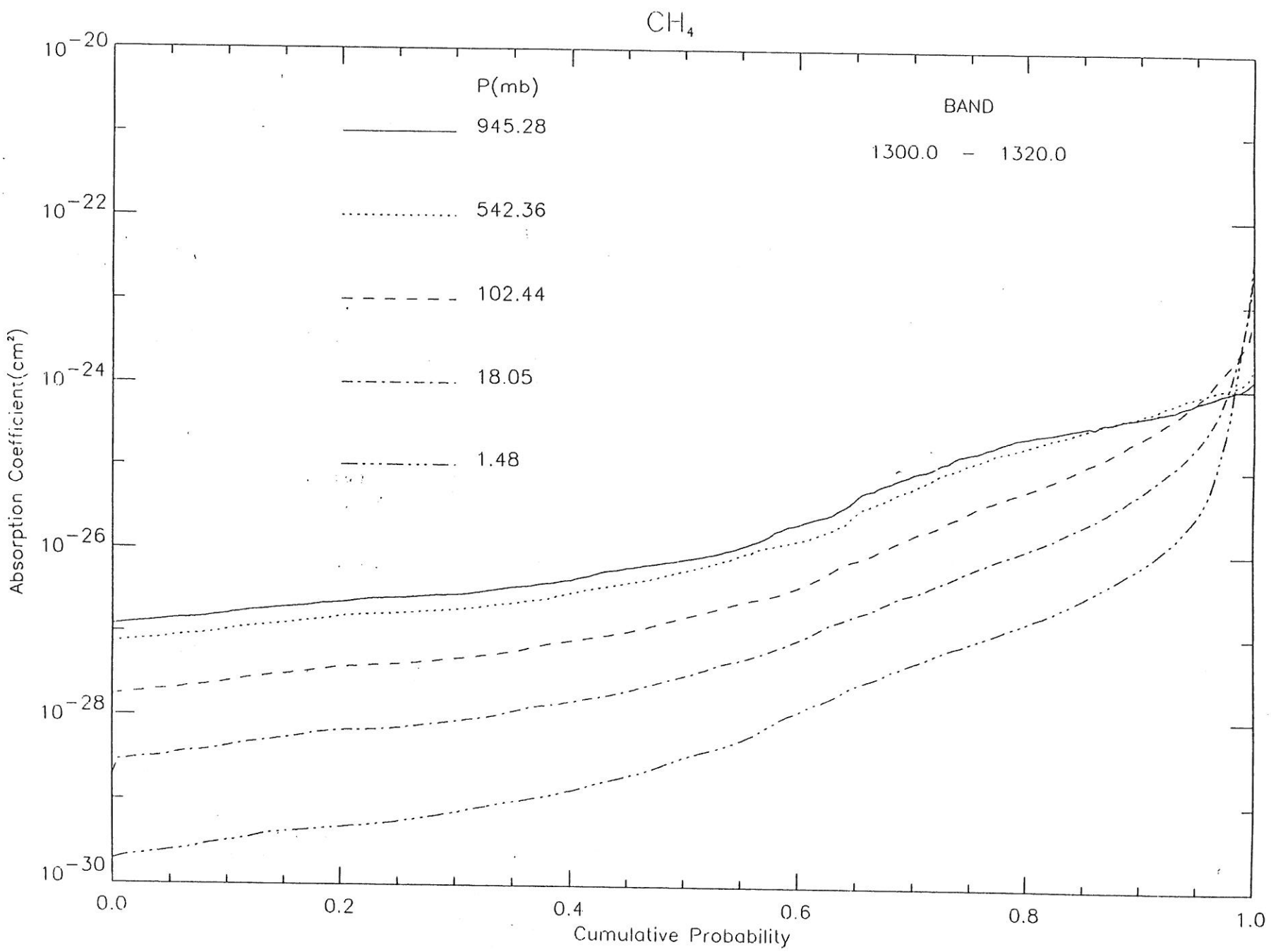
CH_4
P(mb)
945.28
542.36
102.44
18.05
1.48
BAND
1300.0 – 1320.0
Absorption Coefficient(cm²)
10^{-20}
10^{-22}
10^{-24}
10^{-26}
10^{-28}
10^{-30}
0.0
0.2
0.4
0.6
0.8
1.0
Cumulative Probability

Figure 4

TESTS OF ACCURACY OF CORRELATED k's

CH_4 40 points

(vs monochromatic)

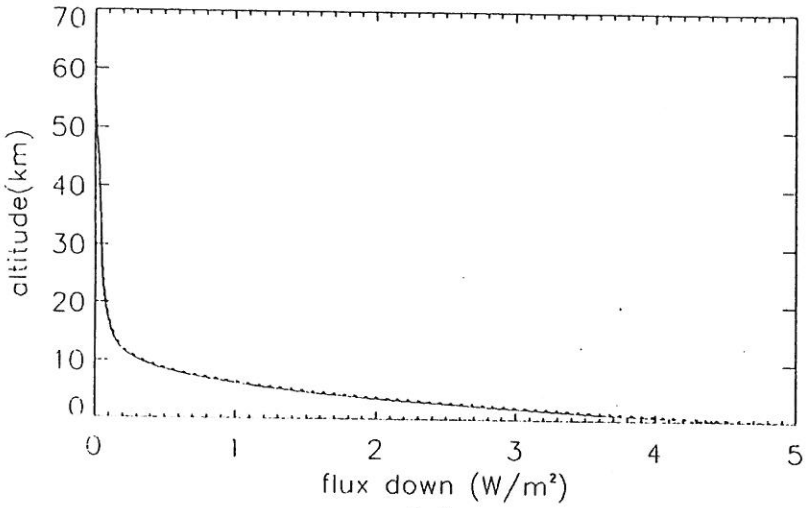

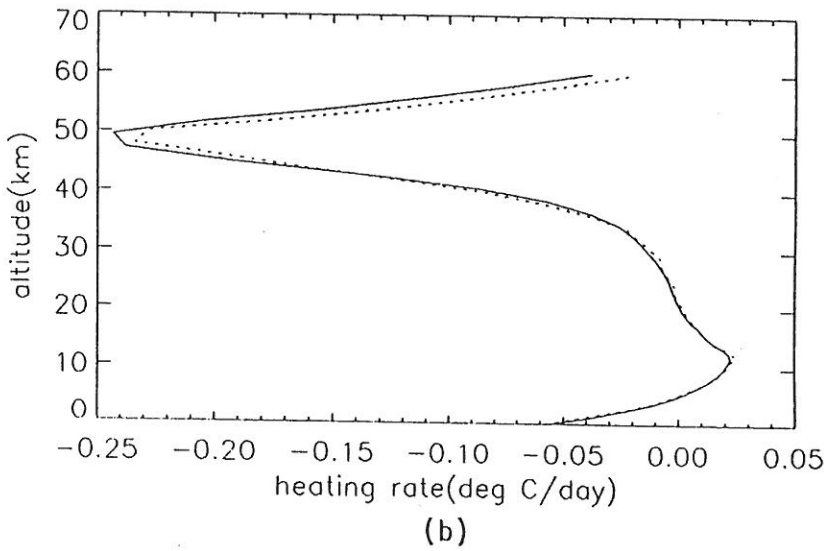

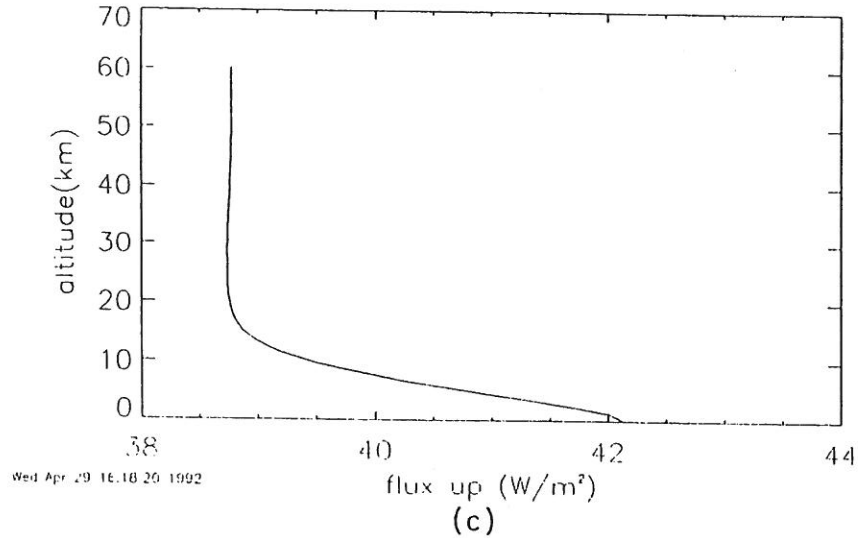

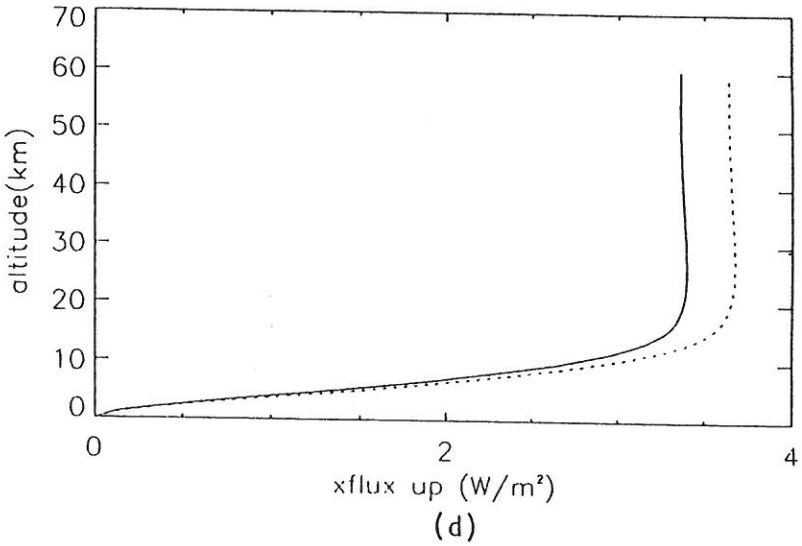

Figure 5

N_2O 40 points

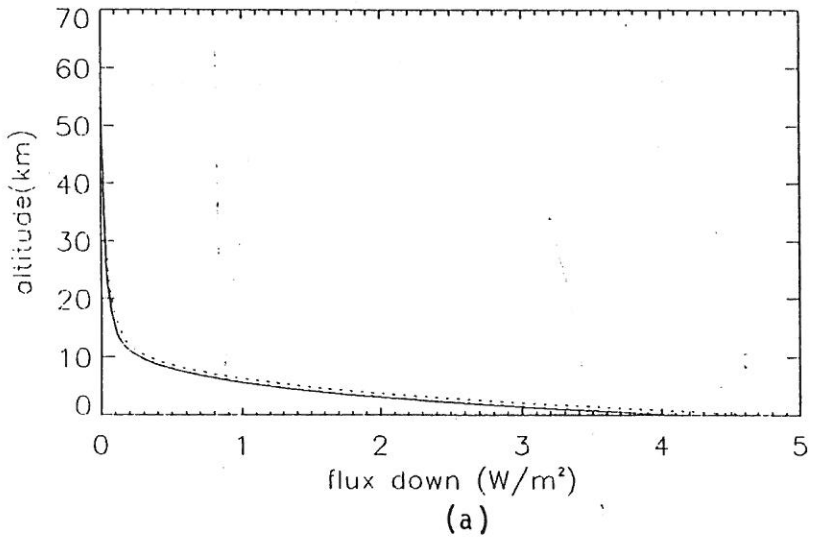

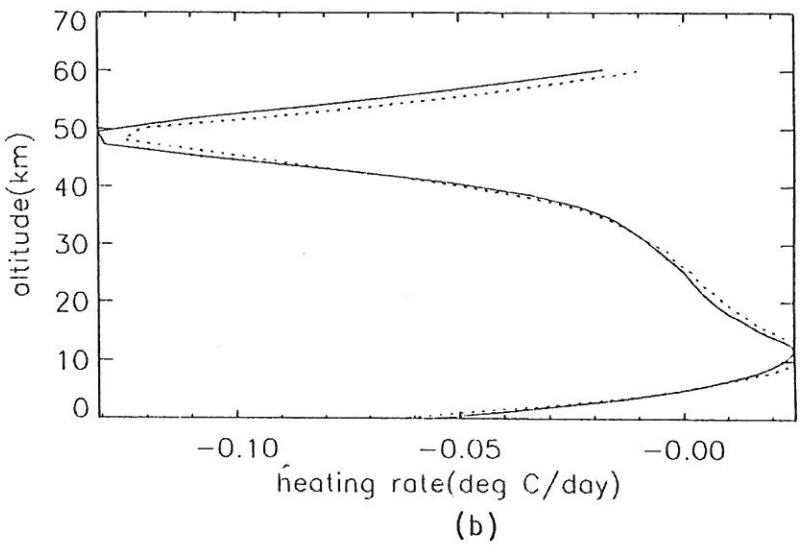

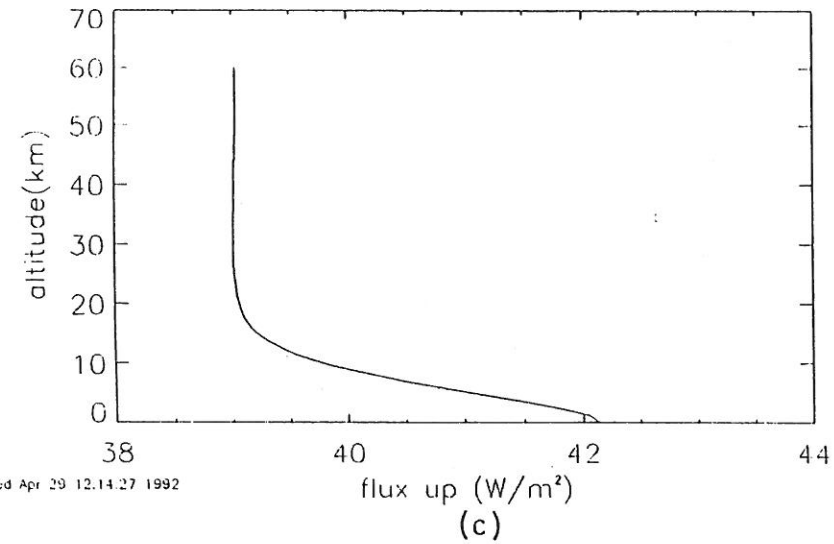

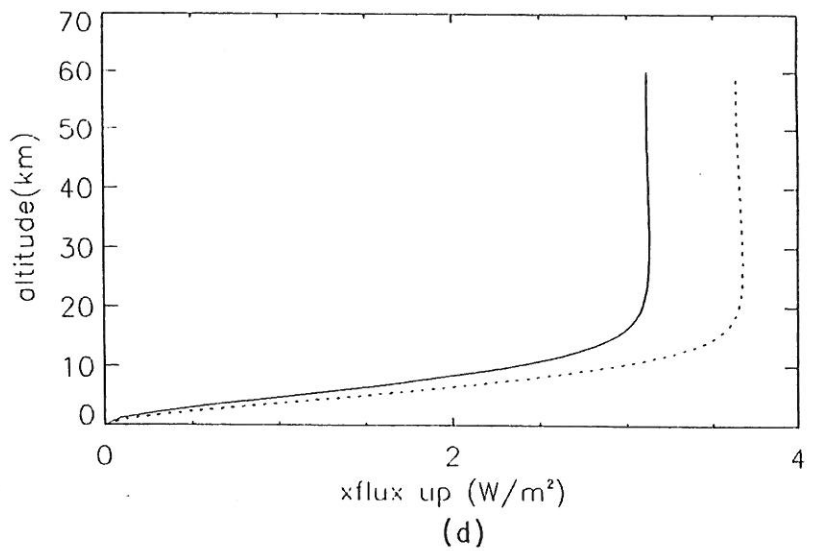

Figure 6

SPECTRAL MAPPING TRANSFORMATION (SMT)

— DEFINITION: WHEN BINNING TOGETHER ~~[illegible]~~ WAVELENGTHS THAT HAVE VERY SIMILAR VALUES OF k, DEMAND THAT THE SIMILARITY HOLD AT ALL P, T LEVELS IN THE ATMOSPHERE

— VS CORRELATED k:

- WITH CORRELATED k WE BIN ONE LEVEL AT A TIME
- SMT MORE ACCURATE FOR INHOMOGENEOUS ATMOSPHERES ($P(z)$, $T(z)$)
- BUT REQUIRES MORE CALCULATIONS PER SPECTRAL INTERVAL (~ 100 – SEVERAL 100 VS 6 – 12 FOR CORRELATED k)
- BETTER ACCURACY ($\leq 1\%$ VS $\leq 5\%$ FOR CORRELATED k + RARE SITUATIONS WITH LARGER ERRORS FOR CORRELATED k.

READING LIST

1. RM Goody + YL Yung, "Atmospheric Radiation, Theoretical Basis" 2nd ed., 1989, Oxford Univ. Press — Chpt. 3 + 5
   (General)
2. Pollack et al. (1993). Near-infrared light from Venus' nightside: a spectroscopic analysis. Icarus, in press.
   (Databases)
3. RA West et al (1990). J. Quantitative Spectrosc. Rad. Transfer, 43, 191-199
   (SMT2)